NASA TECHNICAL NOTE

NASA TN D-8010

NASA TN D-8010

CRACK-CLOSURE AND CRACK-GROWTH MEASUREMENTS IN SURFACE-FLAWED TITANIUM ALLOY Ti-6Al-4V

Wolf Elber

Langley Research Center
Hampton, Va. 23665

NATIONAL AERONAUTICS AND SPACE ADMINISTRATION • WASHINGTON, D. C. • SEPTEMBER 1975

1. Report No.	2. Government Accession No.	3. Recipient's Catalog No.
NASA TN D-8010		

4. Title and Subtitle
CRACK-CLOSURE AND CRACK-GROWTH MEASUREMENTS IN SURFACE-FLAWED TITANIUM ALLOY Ti-6Al-4V

5. Report Date: September 1975

6. Performing Organization Code:

7. Author(s)
Wolf Elber

8. Performing Organization Report No.: L-10099

9. Performing Organization Name and Address
NASA Langley Research Center
Hampton, Va. 23665

10. Work Unit No.: 505-02-31-01

11. Contract or Grant No.:

12. Sponsoring Agency Name and Address
National Aeronautics and Space Administration
Washington, D.C. 20546

13. Type of Report and Period Covered: Technical Note

14. Sponsoring Agency Code:

15. Supplementary Notes

16. Abstract

The crack-closure and crack-growth characteristics of the titanium alloy Ti-6Al-4V were determined experimentally on surface-flawed plate specimens. Under cyclic loading from zero to tension, cracks deeper than 1 mm opened at approximately 50 percent of the maximum load. Cracks shallower than 1 mm opened at higher loads. The correlation between crack-growth rate and the total stress-intensity range showed a "lower threshold" behavior. This behavior was attributed to the high crack-opening loads at short cracks because the lower threshold was much less evident in correlations between the crack-growth rates and the effective stress-intensity range.

17. Key Words (Suggested by Author(s))	18. Distribution Statement
Fatigue Fracture mechanics Crack growth Crack closure Titanium	Unclassified – Unlimited Subject Category 26

19. Security Classif. (of this report)	20. Security Classif. (of this page)	21. No. of Pages	22. Price*
Unclassified	Unclassified	16	$3.25

*For sale by the National Technical Information Service, Springfield, Virginia 22161

CRACK-CLOSURE AND CRACK-GROWTH MEASUREMENTS IN SURFACE-FLAWED TITANIUM ALLOY Ti-6Al-4V

Wolf Elber
Langley Research Center

SUMMARY

The crack-closure and crack-growth characteristics of the titanium alloy Ti-6Al-4V were determined experimentally on surface-flawed plate specimens. Under cyclic loading from zero to tension, cracks deeper than 1 mm opened at approximately 50 percent of the maximum load. Cracks shallower than 1 mm opened at higher loads. The correlation between crack-growth rate and the total stress-intensity range showed a "lower threshold" behavior. This behavior was attributed to the high crack-opening loads at short cracks because the lower threshold was much less evident in correlations between the crack-growth rates and the effective stress-intensity range.

INTRODUCTION

Crack closure during fatigue crack growth under cyclic tension loading was first discovered in thin aluminum sheets (ref. 1). In a later report (ref. 2) it was postulated that a crack can grow only when it is fully open at the crack tip, so that the crack-growth rate should be a function of an effective stress-intensity range. This range is based on the crack-opening stress and the maximum stress in the load cycle. To use such a crack-growth criterion requires precise knowledge of the crack-opening stress during cycling. In reference 2 a compliance method was used to determine the crack-opening stress. The compliance determination was based on crack-opening displacements measured on the surface of specimens just behind the crack tip.

Other methods (refs. 3 to 5) for determining the crack-opening stresses have since been developed and have produced results varying widely from the results in reference 2. No direct comparison can be made among these results because of differences in materials and specimens used in these studies.

These conflicting results have led to a widespread belief that crack-opening stresses are highest in aluminum and in plane-stress crack growth (thin sheets) and that crack-opening stresses are virtually zero under plane-strain crack growth and in titanium.

This study was designed to show whether, in fact, crack closure does occur in titanium alloy Ti-6Al-4V and whether crack closure occurs under plane-strain crack-growth conditions existing during growth of shallow surface flaws. The compliance method was used for that study.

In reference 6, it was shown that residual stresses can strongly influence the growth of surface cracks. To isolate any significant effects of residual stresses in this study, one-half of the specimens tested were prestretched. This process reduces residual stresses in constant-cross-section specimens to insignificant levels.

In crack-growth studies involving "small" crack sizes and "low" stress levels, the stress-intensity range can reach a lower threshold below which no growth occurs. In this study the influence of the crack-opening stresses on this threshold was studied.

SYMBOLS

a	depth of semicircular crack, m
a_1, a_2	successive values of crack depth, m
C	constant in crack-growth law
$\frac{da}{dN}$	crack-growth rate, m/cycle
K	stress-intensity factor, $N/m^{3/2}$
ΔK	total stress-intensity range, $N/m^{3/2}$
ΔK_{eff}	effective stress-intensity range, $N/m^{3/2}$
M_e	geometric magnification factor
n	exponent in crack-growth law
N	number of load cycles
Q	shape factor for surface cracks
S	gross section stress, Pa

S_{max} maximum gross section stress, Pa

S_{min} minimum gross section stress, Pa

S_{op} crack-opening stress, Pa

U Effective stress ratio

PROCEDURE

Specimens

The test specimen configuration is shown in figure 1. The semicircular crack starters of 0.6-mm radius were machined with an electroerosion process. The specimen thickness (10 mm) was chosen so that cracks could be grown to about 10 times their initial depths while under essentially plane-strain conditions. Target holes for the crack-opening displacement (COD) gage were machined above and below the center of the notch. (See detail B, fig. 1.)

Material

The titanium Ti-6Al-4V used for this study was mill annealed and grit blasted. It had a Young's modulus of 103 GPa, nominal tensile strength of 964 MPa, and an elongation of 12 percent in 50 mm.

Testing

Six specimens were tested under constant-amplitude cyclic loading from zero to tension. Before the crack starters were machined, three specimens were preloaded to a permanent strain of 0.2 percent to remove any residual stresses left by the grit blasting. Such residual stresses from surface treatments can influence the crack-growth behavior (ref. 6). Three cyclic stress amplitudes were selected, covering the typical range of stresses for aerospace structural applications. The testing frequencies were determined by the response limitations of the servohydraulic fatigue-testing machine. The test parameter matrix is shown in table I. Each test was stopped when the total displacement reached the measurement range of the COD gage.

Measurements

The COD gage was mounted over the center of the crack starter during the entire test, and the load-displacement curve was monitored continuously on an oscilloscope screen. Precise load and displacement measurements were taken whenever the monitor

indicated that the compliance had increased 20 percent over the previous reading. To obtain accurate measurements, the loading frequency was slowed to one-hundredth of the normal testing frequency. The load and corresponding displacement signals were passed into a data acquisition system for compliance analysis. Crack depths were calculated from the compliance data and the gage calibration (ref. 6).

Determination of Crack-Opening Load

During each measurement load cycle the data acquisition system takes 150 successive readings of load and corresponding crack-opening displacement. These data sets are stored on magnetic tape for later analysis. During that analysis, the data are scanned for identification of one complete load cycle and the location of the maximum load; then the maximum elastic compliance is calculated from the first 10 readings after the maximum load. This compliance value is used both to calculate crack depths and to determine reduced displacements. Reduced displacements are defined herein as the differences between the measured displacements and the least-squares line fit through the 10 load-displacement points following the maximum load. The advantage of the reduced displacements is that they have increased resolution for graphical determination of the crack-opening load.

A computer plots both the load-displacement data and the load–reduced-displacement data. A typical plot is shown in figure 2. According to the compliance method of crack-opening determination (ref. 2), the crack opens fully during the loading portion of the cycle when the compliance reaches the value which was obtained immediately after the maximum load on the unloading portion of the previous cycle. On the reduced-displacement plot the crack is interpreted to be fully open when the tangent to the loading curve becomes vertical which, as shown in figure 2, is at approximately 45 percent of the maximum load.

RESULTS AND DISCUSSION

Crack Growth

The crack-growth curves for the six specimens are shown in figure 3, and the experimental data (crack depths and cycles) are listed in table II. At all three stress levels, cracks grew faster in the prestretched material than in the as-received material. The largest difference in growth rate occurred at the lowest stress level and at small crack depths (less than 1 mm).

The crack-growth rate between two successive crack-depth readings a_1 and a_2 is defined as

$$\frac{da}{dN} = \frac{a_2 - a_1}{N_2 - N_1}$$

at crack depth

$$a = \frac{a_1 + a_2}{2}$$

The stress used as a correlating function in the crack-growth-rate equations is given by

$$K = S\sqrt{\pi a}\,\frac{M_e}{\sqrt{Q}}$$

where M_e and Q are dimensionless correction factors related to the configurations of the specimen and the surface crack, respectively (ref. 7). Examination of the fracture surfaces showed that the crack shapes remained semicircular throughout the tests, so that M_e and Q were constant. The calculated stress intensities are plotted against the crack-growth rates in figure 4, with specimens grouped according to stress level. The equation for crack growth is assumed to be

$$\frac{da}{dN} = C(\Delta K)^n$$

where $C = 3.34 \times 10^{-13}$ and $n = 4.78$, which were determined from a least-squares fit to the data.

At all three stress levels the crack-growth rate approaches zero at some finite value of stress-intensity range. This value is referred to later as the apparent lower threshold of crack growth. The small differences between growth rates for the prestretched and as-received material occurred mainly at low stress levels and small crack depths (less than 1 mm). This indicates that the residual stresses in the as-received material are small and concentrated near the surface. The numerical values of the crack-growth-rate data points are listed in table II.

Crack-Opening Loads

All data were analyzed to obtain the effective stress ratio, which is defined as

$$U = \frac{S_{max} - S_{op}}{S_{max} - S_{min}} \qquad \left(S_{op} > S_{min}\right)$$

The parameter U is plotted against crack depth a for all six specimens in figure 5. The numerical values of the data points are given in table II.

For each specimen the effective stress ratio is initially small but increases rapidly as the crack begins to grow out of the influence of the initial crack starter. However, there is no general trend in U for cracks deeper than 1 mm. For the 67 data points

analyzed, the mean is $U = 0.50$ with a standard deviation of 0.11; that is, the mean crack-opening load is approximately one-half of the maximum load for loading from zero to tension.

Effective Stress—Crack-Growth Law

The crack-growth rate data were correlated with the effective stress-intensity range according to the rate equation

$$\frac{da}{dN} = C(\Delta K_{eff})^n = C(U\Delta K)^n$$

where $C = 1.07 \times 10^{-10}$ and $n = 3.52$ for the least-squares line for all the data points.

The experimental curves of all six data sets are shown in figure 6, with the data sets grouped according to stress level. Generally, the data show greater scatter (deviation of data points from a smooth curve) than the basic data of figure 4. The greater scatter is caused by the scatter in the measured values of the effective stress ratio U. However, the lower threshold, which is evident in plots of the crack-growth rate and the total stress-intensity range, is not evident in plots of the crack-growth rate and the effective stress-intensity range. Therefore, the lower threshold can be attributed primarily to the crack-closure behavior, which is governed by the distribution of residual deformations left behind the crack.

CONCLUDING REMARKS

The crack-closure analysis of surface-flawed titanium alloy Ti-6Al-4V under cyclic loading from zero to tension shows that crack closure occurred in the titanium under the plane-strain conditions. For crack depths in excess of 1 mm the crack-opening levels were independent of crack depth and cyclic stress levels. Cracks opened at about 50 percent of the maximum loads. For crack depths less than 1 mm the crack-opening stress levels were even higher, resulting in smaller effective stress ranges and extremely small crack-growth rates just after initiation.

The differences between crack-growth rates in prestretched and as-received material were small for cracks deeper than 1 mm. This shows that residual stresses in the as-received material affected crack growth only in the initiation phase.

In correlations between crack-growth rates and the total stress-intensity range, apparent lower thresholds were observed at all stress levels; a power law does not describe these data adequately. However, when crack-growth rates were correlated with

effective stress-intensity range, a good power-law correlation was obtained. The apparent thresholds hence were attributed to the rapid increase in effective stress ratio initiation.

Additional work is required to establish the relation between the effective stress ratio and the ratio of minimum stress to maximum stress for this titanium alloy.

Langley Research Center
National Aeronautics and Space Administration
Hampton, Va. 23665
June 30, 1975

REFERENCES

1. Elber, Wolf: Fatigue Crack Closure Under Cyclic Tension. Eng. Fracture Mech., vol. 2, no. 1, July 1970, pp. 37-45.

2. Elber, Wolf: The Significance of Fatigue Crack Closure. Damage Tolerance in Aircraft Structures. Spec. Tech. Publ. 486, American Soc. Testing & Mater., 1971, pp. 230-242.

3. Shih, T. T.; and Wei, R. P.: A Study of Crack Closure in Fatigue. NASA CR-2319, 1973.

4. Roberts, R.; and Schmidt, R. A.: Observations of Crack Closure. Int. J. Fracture Mech., vol. 8, no. 4, Dec. 1972, pp. 469-471.

5. Buck, Otto; Ho, C. L.; Marcus, H. L.; and Thompson, R. B.: Rayleigh Waves for Continuous Monitoring of a Propagating Crack Front. Stress Analysis and Growth of Cracks, Spec. Tech. Publ. 513, American Soc. Testing & Mater., 1972, pp. 280-291.

6. Elber, Wolf: Effects of Shot-Peening Residual Stresses on the Fracture and Crack-Growth Properties of D6AC Steel. Fracture Toughness and Slow-Stable Cracking. Spec. Tech. Publ. 559, American Soc. Testing and Mater., 1974, pp. 45-58.

7. Newman, J. C., Jr.: Fracture Analysis of Surface- and Through-Cracked Sheets and Plates. Eng. Fracture Mech., vol. 5, no. 3, Sept. 1973, pp. 667-689.

TABLE I.- TEST MATRIX

Specimen	Preload strain, percent	Cyclic maximum stress, N/mm^2	Testing frequency, Hz
1	0.2	413	3.5
2	.2	551	3.0
3	.2	689	2.5
4	0	689	2.5
5	0	551	3.0
6	0	413	3.5

TABLE II.- RESULTS FROM TESTS AND CALCULATIONS

Specimen	Stress, MPa	Crack depth, mm	Cycles	Effective stress ratio	Stress intensity, $MN/m^{3/2}$	Crack-growth rate, m/cycle
1	413.1	0.54	1 500	0.35		
		.58	14 279	.50	7.2	2.750E-9
		.64	24 182	.45	7.5	6.111E-9
		.76	33 600	.45	8.1	1.306E-8
		1.35	46 200	.40	9.9	4.710E-8
		1.63	48 300	.40	11.8	1.292E-7
		3.38	54 260	.40	15.3	2.935E-7
		4.80	56 000	.50	19.5	8.190E-7
		5.65	56 636	.45	22.1	1.335E-6
6	413.1	0.52	0	0.30		
		.55	11 500	.50	7.1	3.141E-9
		.61	41 420	.50	7.4	1.762E-9
		.63	48 800	.50	7.6	3.439E-9
		.66	53 800	.45	7.8	6.442E-9
		.77	66 500	.45	8.2	8.608E-9
		1.09	85 000	.45	9.3	1.688E-8
		1.44	92 000	.45	10.8	4.992E-8
		1.70	94 750	.40	12.1	9.477E-8
		2.31	98 368	.40	13.7	1.700E-7
		2.88	100 481	.40	15.6	2.679E-7
		3.45	102 000	.47	17.2	3.791E-7
		4.52	103 812	.45	19.3	5.872E-7
		5.74	105 056	.40	21.9	9.808E-7
		6.08	105 330	.45	23.5	1.247E-6
2	551.0	0.58	0	0.30		
		.79	10 000	.50	10.7	2.011E-8
		1.43	13 820	.60	13.6	1.694E-7
		1.91	15 115	.65	16.7	3.693E-7
		2.42	16 065	.65	18.9	5.343E-7
		2.71	16 514	.65	20.6	6.522E-7
		3.49	17 322	.65	22.7	9.665E-7
		4.44	18 000		25.6	1.397E-6

TABLE II.- RESULTS FROM TESTS AND CALCULATIONS – Concluded

Specimen	Stress, MPa	Crack depth, mm	Cycles	Effective stress ratio	Stress intensity, $MN/m^{3/2}$	Crack-growth rate, m/cycle
5	551.0	0.58	4 000	0.40		
		.62	7 800	.50	10.0	1.259E-8
		.71	10 480	.50	10.5	3.059E-8
		.83	12 360	.45	11.3	6.802E-8
		.96	13 800	.55	12.2	8.948E-8
		1.15	15 010	.60	13.2	1.509E-7
		1.37	16 210	.60	14.4	1.871E-7
		1.79	17 645	.50	16.2	2.952E-7
		2.32	18 900	.65	18.5	4.135E-7
		3.22	20 250	.65	21.4	6.695E-7
		4.47	21 320	.60	25.2	1.168E-6
3	689.0	0.54	0	0.20		
		.56	2 700	.40	11.9	8.315E-9
		.61	3 500	.55	12.3	6.589E-8
		.73	4 700	.60	13.2	9.761E-8
		.86	5 561	.65	14.3	1.474E-7
		1.00	6 263	.55	15.5	2.086E-7
		1.33	7 242	.50	17.4	3.290E-7
		1.75	8 125	.50	20.0	4.753E-7
		2.16	8 775	.55	22.5	6.457E-7
		2.72	9 335	.50	25.2	9.936E-7
		3.58	9 924	.50	28.6	1.458E-6
		4.38	10 279	.55	32.1	2.255E-6
4	689.0	0.55	1	0.20		
		.56	2 000	.30	12.0	5.860E-9
		.57	3 000	.60	12.1	1.074E-8
		.58	4 000	.62	12.2	1.659E-8
		.60	5 000	.60	12.4	1.952E-8
		.66	6 100	.64	12.8	4.881E-8
		.74	7 000	.60	13.5	9.327E-8
		.88	8 000	.60	14.5	1.347E-7
		1.07	9 000	.55	15.9	1.942E-7
		1.33	9 800	.60	17.6	3.185E-7
		1.61	10 577	.60	19.5	3.643E-7
		1.90	10 800	.60	21.3	1.313E-6

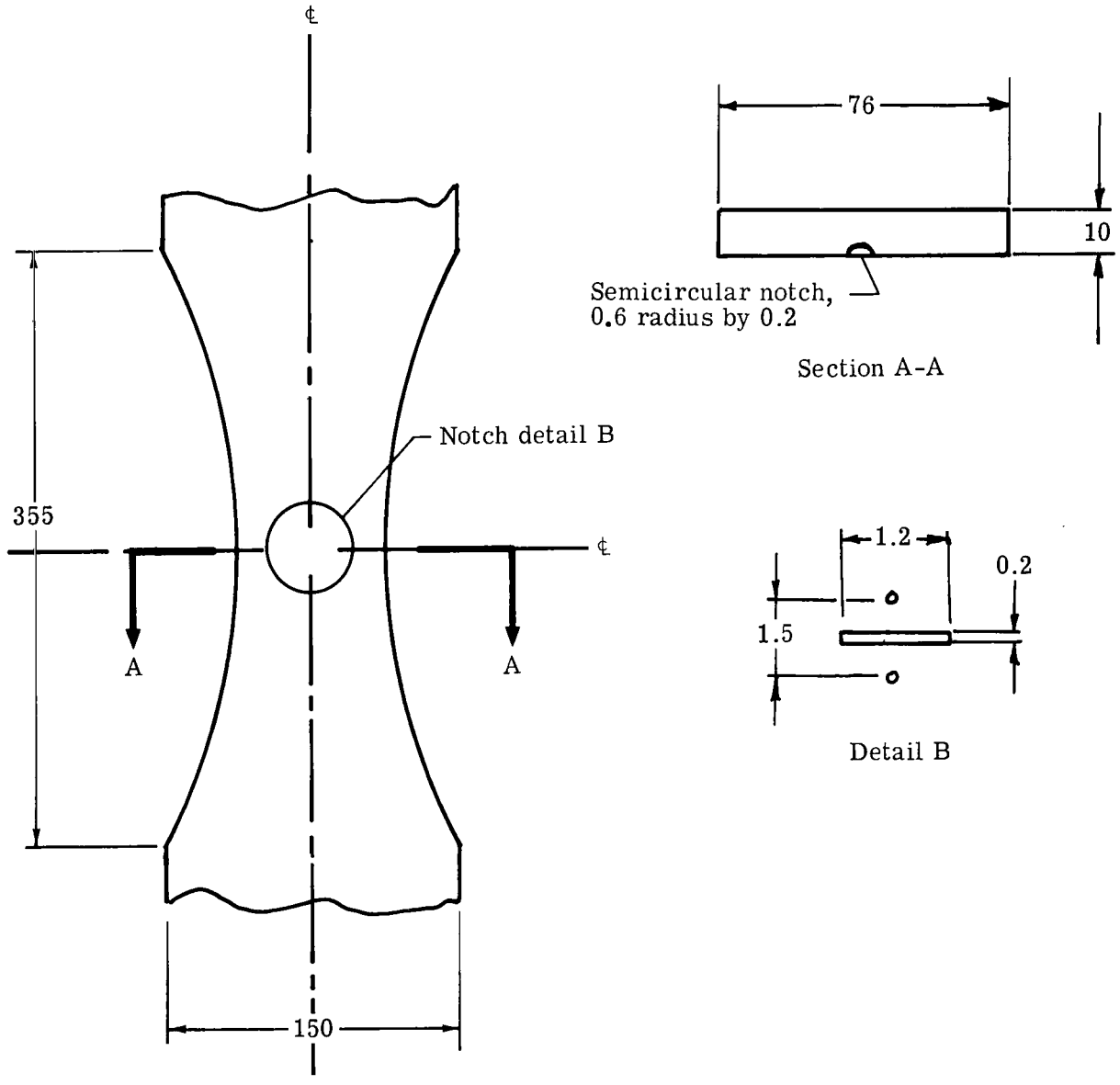

Figure 1.- Test specimen configuration. All dimensions are in mm.

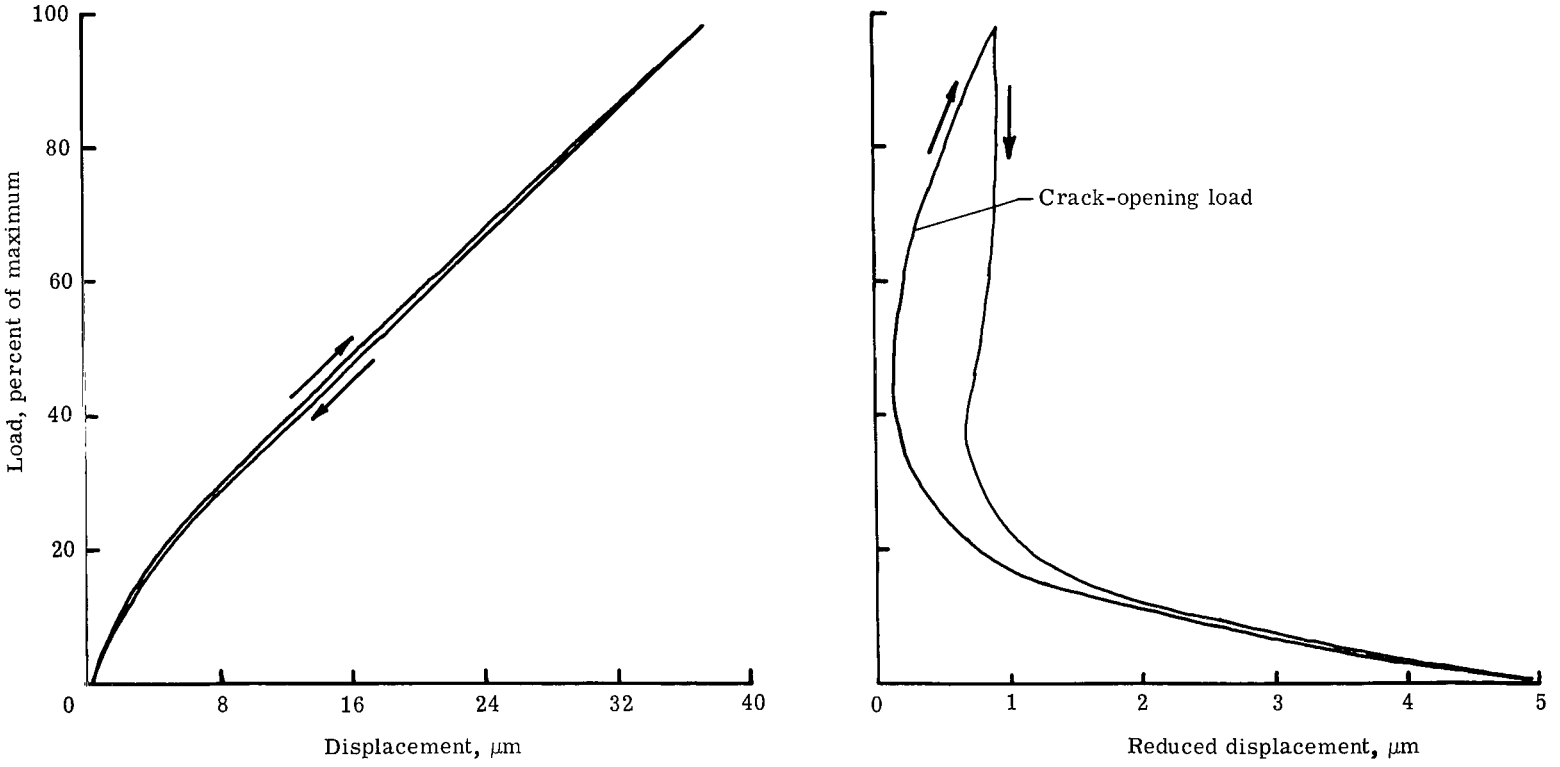

(a) Load-displacement relation.

(b) Load—reduced-displacement relation.

Figure 2.- Load-displacement relations for specimen 4 at crack depth of 1.07 mm. Crack opening occurs at 45 percent of maximum load.

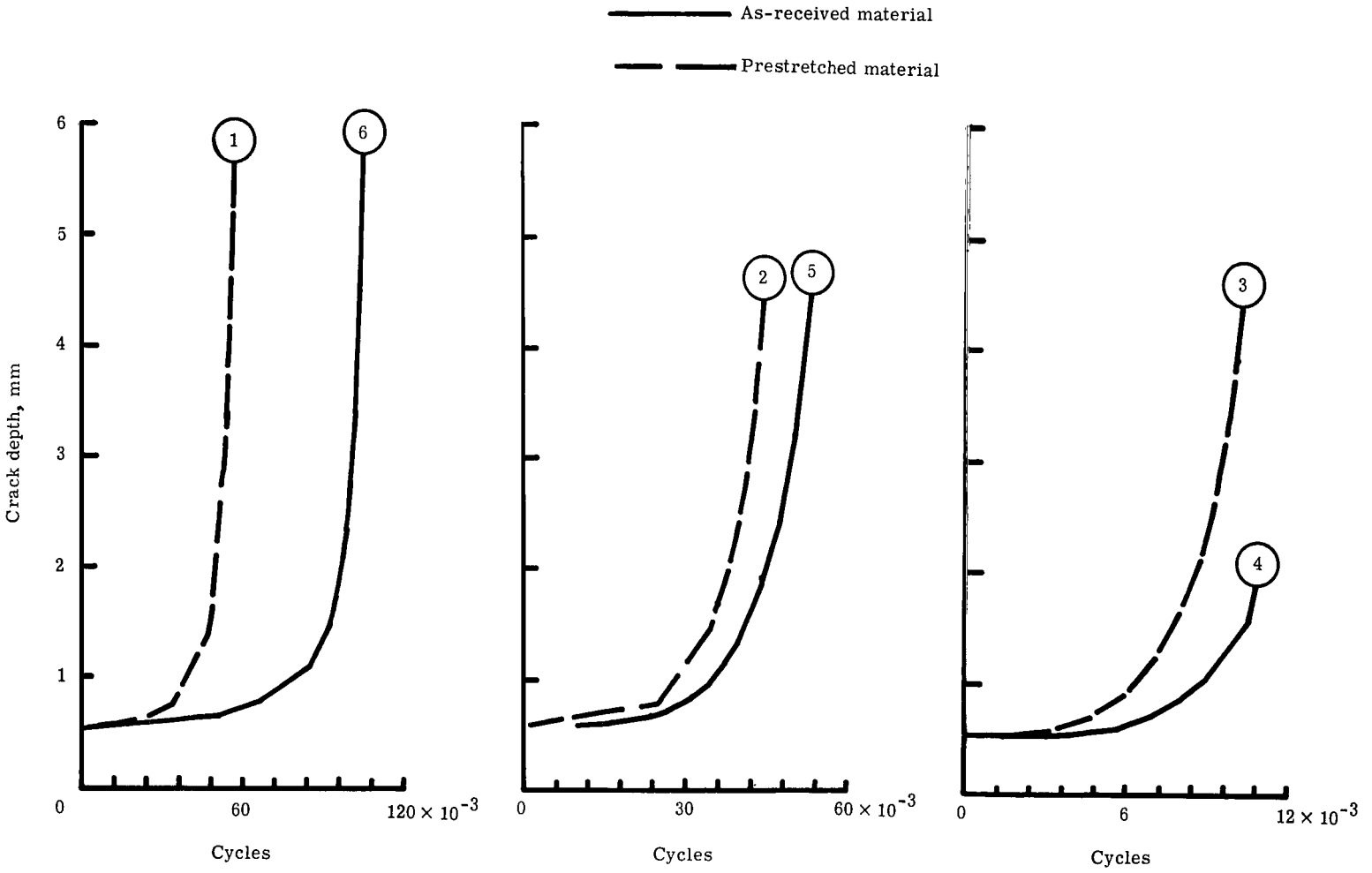

(a) S_{max} = 413.0 MPa. (b) S_{max} = 551.0 MPa. (c) S_{max} = 689.0 MPa.

Figure 3.- Relation between crack depth and cycles. Specimen numbers are indicated in circles.

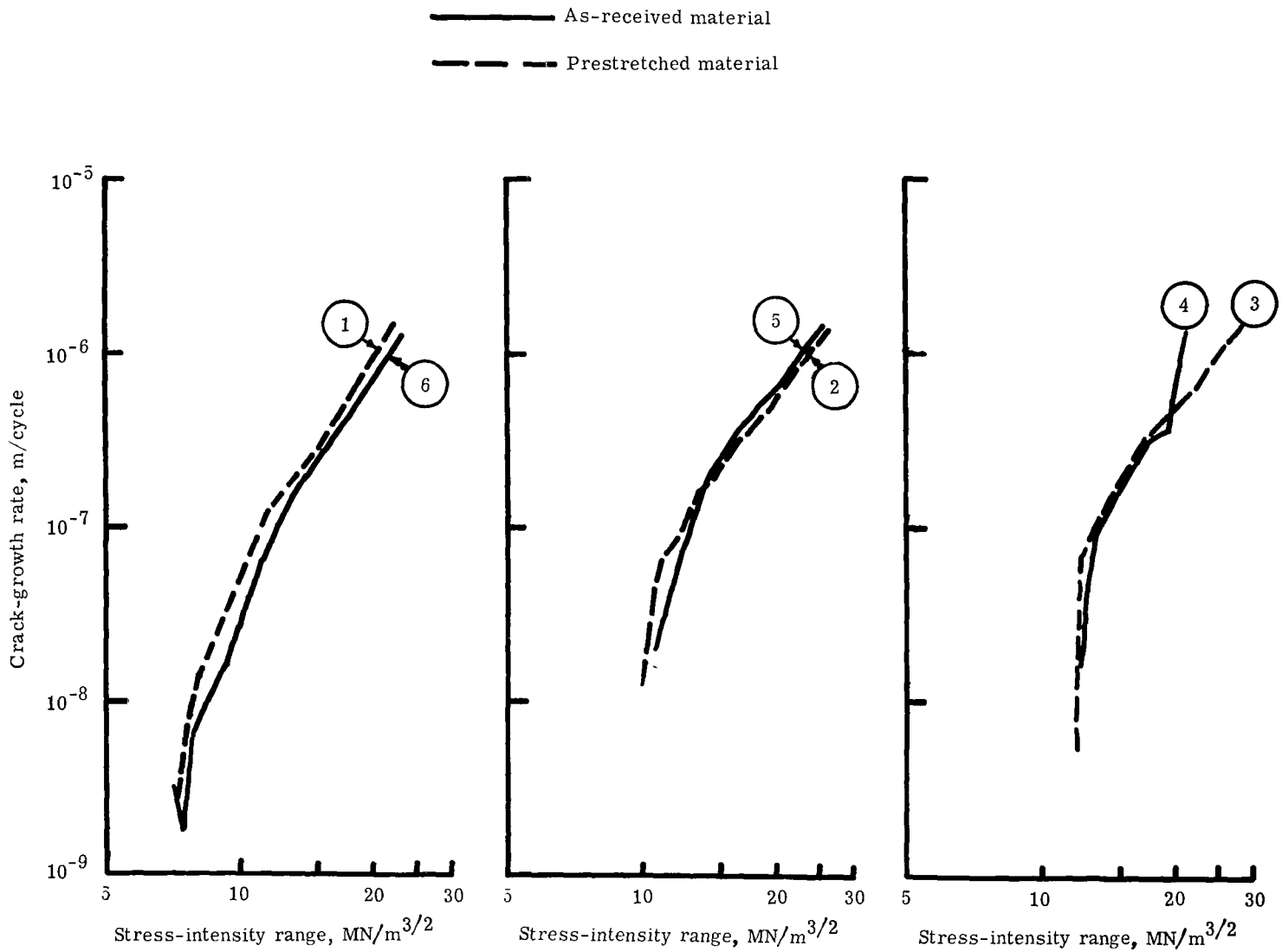

(a) S_{max} = 413.1 MPa. (b) S_{max} = 551.0 MPa. (c) S_{max} = 689.0 MPa.

Figure 4.- Relation between crack-growth rate and stress-intensity range.
Specimen numbers are indicated in circles.

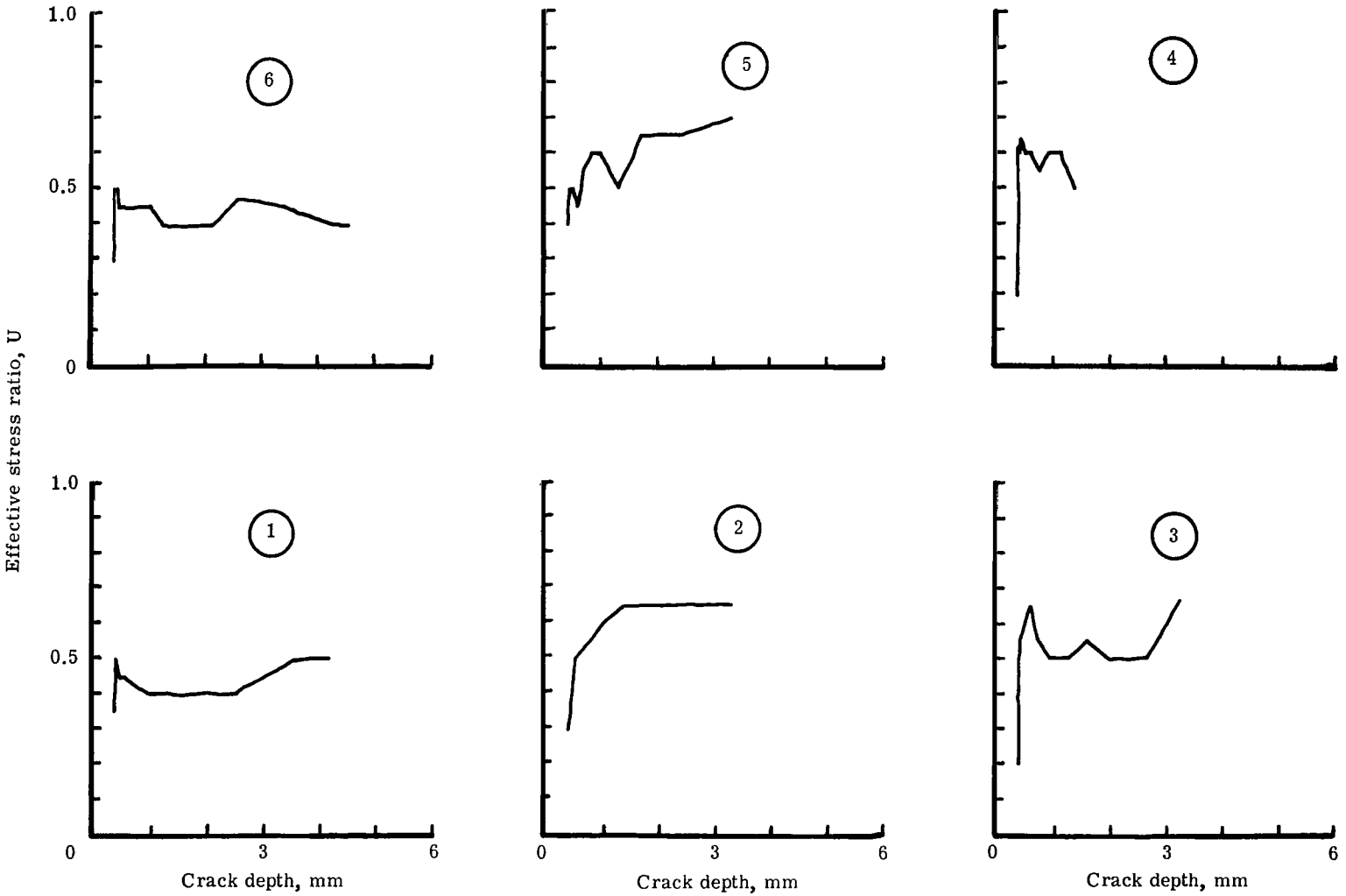

(a) S_{max} = 413.1 MPa. (b) S_{max} = 551.0 MPa. (c) S_{max} = 689.0 MPa.

Figure 5.- Relation between effective stress ratio and crack depth. Specimen numbers are indicated in circles.

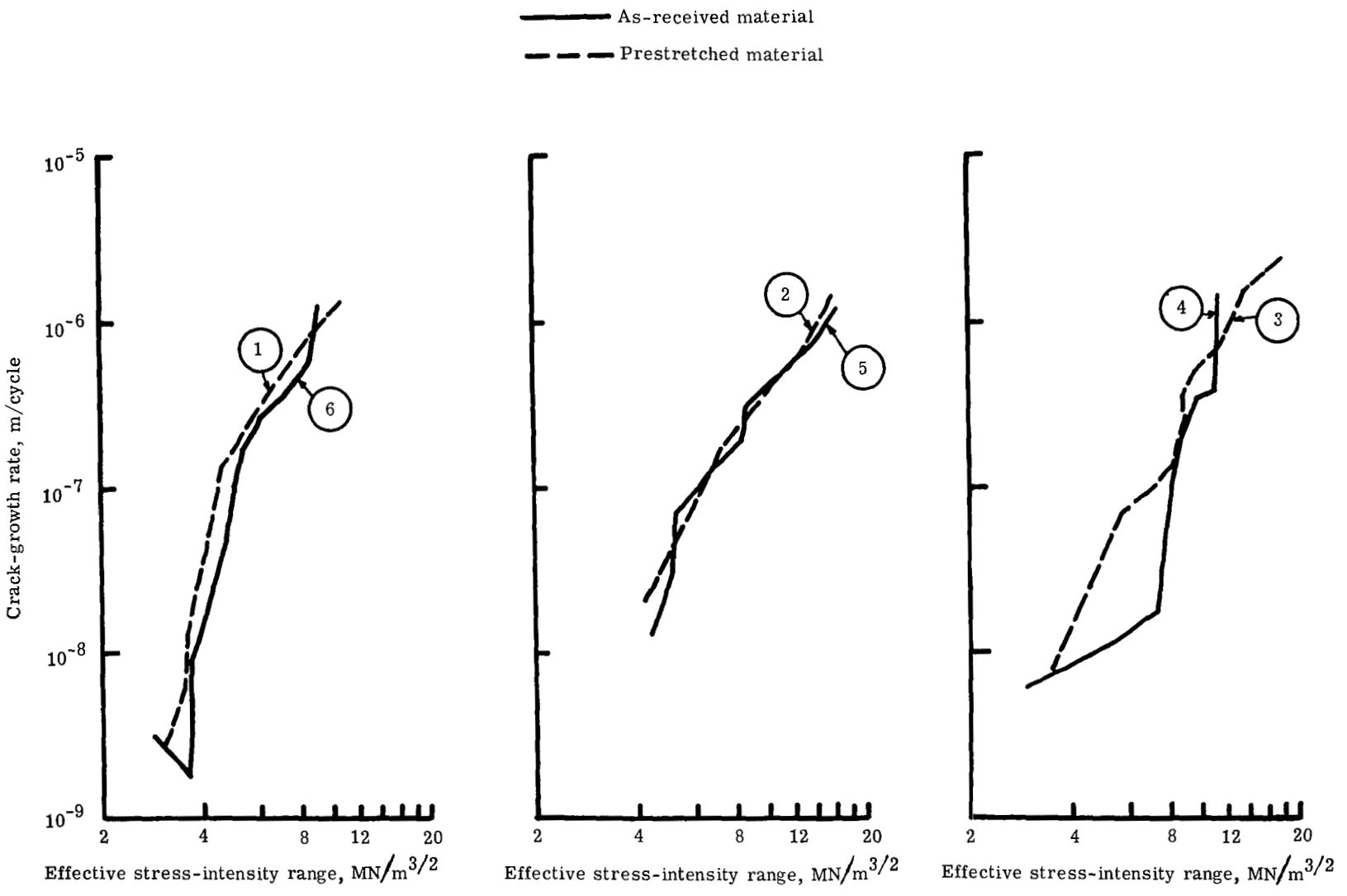

(a) S_{max} = 413.1 MPa. (b) S_{max} = 551.0 MPa. (c) S_{max} = 689.0 MPa.

Figure 6.- Relation between crack-growth rate and effective stress-intensity range. Specimen numbers are indicated in circles.